Dielectric Elastomer Multi-Sensors and Tactile Actuators for Robot Fingers in Human-Robot Interaction

Seiki Chiba * and Mikio Waki

Posted Date: 4 July 2023

doi: 10.20944/preprints202307.0181.v1

Keywords: dielectric elastomer; sensor; actuator; vibrator; stretch; pressure; large deformation; CNT spray; load cells; SS curve

Article

Dielectric Elastomer Multi-Sensors and Tactile Actuators for Robot Fingers in Human-Robot Interaction

Seiki Chiba [1,*] and Mikio Waki [2]

[1] CEO, Chiba Science Institute, Yagumo, Meguro ward, Tokyo 152-0023 Japan
[2] Wits Inc., Oshiage, Sakura, Tochigi, 329-1334, Japan; waki@wits-web.com
* Correspondence: epam@hyperdrive-web.com

Abstract: Conventional sensors used to measure properties such as deformation or pressure, etc. often make use of metals, ceramics, piezos, and other materials. Many of those materials are very hard, so if they are used as sensors, when the object is deformed, or when the pressure on the object changes from time to time, it is necessary to prepare a variety of sensors with different properties. In this experiment, a dielectric elastomer (DE) pressure sensor was fabricated using a hydrogenated nitrile rubber (HNBR) film with improved hardness and elongation. With this, even very thin film (0.2mm) can be measured at any pressure between 1gf and 20kgf. Previously developed film was harder and less stretchy than the current one, with a pressure detection width from 4 kgf to 120 kgf. This time, however, the pressure sensitivity of the finger has been made more sensitive, making it possible to measure even smaller values. A DE stretch sensor was also developed using single-walled carbon nanotube (SWCNT) electrodes with larger stretchability and flexibility, utilizing this HNBR. This greatly improved the mechanical flexibility and stretchability of the DES. Using this stretch sensor, it became possible to sense the motion of the robot's fingers, and to sense the force (pressure) when the fingertip touched the target object with the DE pressure sensor. In addition, it was confirmed that the sensation of the robot's finger touching an object can be fed back to a human finger by using a small diaphragm type vibrator DE actuator.

Keywords: dielectric elastomer; sensor; actuator; vibrator; stretch; pressure; large deformation; CNT spray; load cells; SS curve

1. Introduction

Some composite materials that can be utilized as sensor materials are piezoelectric composite materials [1], conductive polymer materials [2], bimetals [3], and others. The first two are materials that combine the advantages of both organic and inorganic materials in a matrix. The others are used in temperature sensors, and others devices, by combining dissimilar metals. In addition, for engineering sensors, using materials such as new metal materials (e.g., liquid metal), high-performance polymer materials, fine ceramics, composite materials based on additive manufacturing, and others combined with electronics and biotechnology, may be able to meet various needs in the 21st century. They are expected to be used in cutting-edge technologies that supporting a variety of industries and economies [4,5]. Examples include robotics, wearable electronics [6], epidermal electronic systems [7], human-machine interfaces [8], soft robotics [9], other biomedical devices [10, 11], and related systems [12]. In most of these systems, sensory feedback plays an important role in considering efficiency and performance accuracy. Tactile sensors currently in use include pressure [13], strain [14], shear [15], force [16, 17] and vibration sensors [18]. Through contact between objects and their sensors,human contact perception can be emulated in robots, and other machines. Common transduction principles used in this type of sensor include piezoresistive, piezocapacitive, piezoelectric, and triboelectric [19]. However, those materials are hard, and their mechanical flexibility and stretchability need to be improved.

Preprints (www.preprints.org) | NOT PEER-REVIEWED | Posted: 4 July 2023 doi:10.20944/preprints202307.0181.v1

One of the goals of the experiments was to increase the finger's pressure sensitivity more sensitive and measure even smaller values. Additionally, the development of a DE stretch sensor with greater stretchability and flexibility using single-walled carbon nanotube (SWCNT) electrodes and this HNBR was attempted, in order to significantly improve the mechanical flexibility and stretchability of the DE sensors. Furthermore, using this stretch sensor, an experiment to sense the movement of the robot's finger and detect the force (pressure) when the fingertip touched the target object with the DE pressure sensor was tried. An experiment using a small diaphragm-type transducer DE actuator to confirm that the sensation of a robot finger touching an object can be fed back to a human finger was also conducted.

2. Background of Dielectric Elastomers

Dielectric elastomer (DE) was developed starting in 1991 by S. Chiba, R. Pelrine et al. at the Stanford Research Institute (SRI International, USA) [20,21]. The DE can be an actuator, a sensor and a generator with the same structure [22]. Chiba et al. demonstrated that a 0.15 g DE could lift an 8 kgf weight by more than 1 mm in 88 ms, and they also demonstrated the great potential of ultra-lightweight and ultra-high performance DE motors [22,23]. They also developed a portable DE generator and showed that it is possible to charge a secondary battery at the same time [24].

The development of artificial muscles by chemical approaches began in 1949 with actuators that depended on the movement of ions in polymer gels [25,26]. Actuators using ionic polymer-metal composites or conducting polymers utilize force by electrically transferring ions within the polymers [27, 28]. In addition, actuators utilizing carbon nanotubes (CNT), heat, light, liquid crystal, air, and shape memory alloys are currently in development [29–36]. However, since it is superior in terms of performance, DE is becoming the mainstream. Piezo elements can generate a large force to some extent, and so actuators using piezo elements are in development. However, the element itself is hard and stretches little, so it is hard to call it a muscle [37].

The structure of the DE is simple, consisting of an actuator sandwiched between flexible electrodes above and an elastomer (polymer) below. When a voltage is applied to the electrodes, the upper and lower electrodes are attracted by the Coulomb force and the elastomer is crushed, resulting in lateral elongation of the elastomer, forming a linear actuator that changes up to 680% [23,38]. The structure and principle of a DE sensor (DES) (see Figure 1) is the same as a DE actuator (DEA), and the drive principle is inversely proportional to DEA output and elongation. Also, the change in capacitance and its elongation in DES and DEA are directly proportional (see Figure 2).

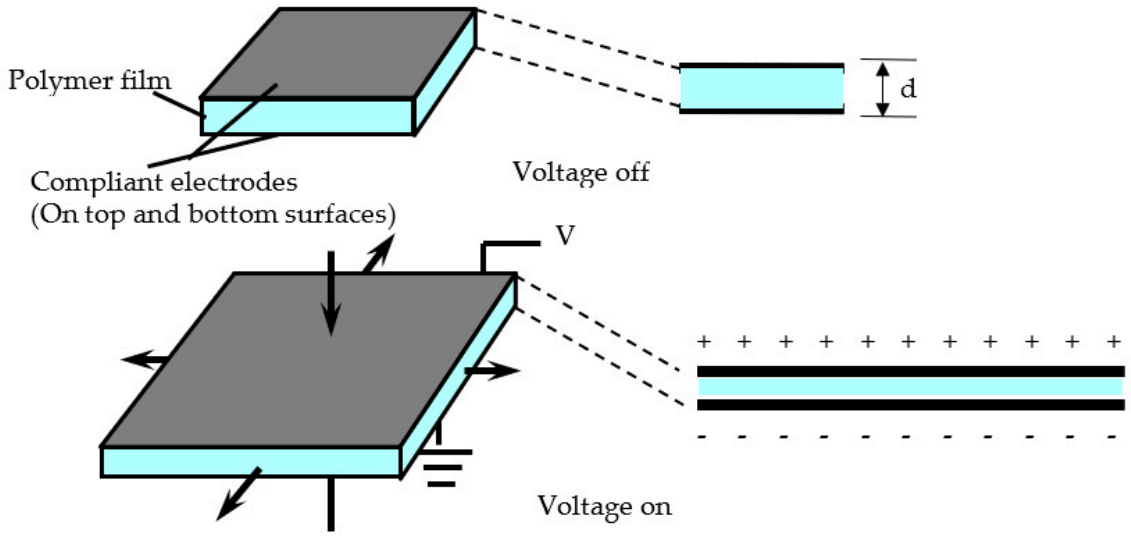

Figure 1. Structure and principle of DES.

Preprints (www.preprints.org) | NOT PEER-REVIEWED | Posted: 4 July 2023 doi:10.20944/preprints202307.0181.v1

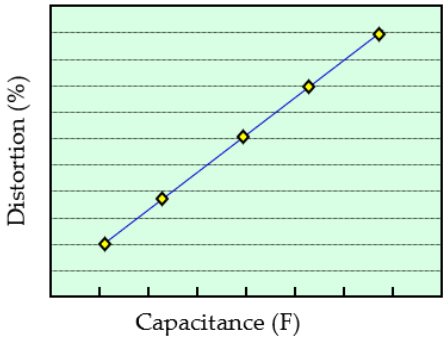

Figure 2. Relationship between the elongation of the DES and capacitance.

The relationship between DES and capacitance can be expressed by the following simple equation:

$$C = \varepsilon \varepsilon_o S/d \quad (1)$$

where, C is the capacitance (F), ε and ε_o are the permittivity of free space and the relative permittivity (dielectric contact) of the polymer, respectively (F/m), S is the electrode area (m^2), and d is the distance between the electrodes (m).

Also, the changed area can be obtained from the following formula.

$$S = Cd/ \varepsilon \varepsilon_o \quad (2)$$

The elongation, l is

$$lw = Cd/ \varepsilon \varepsilon_o \quad (3)$$

where l is the length of the DES and w is its width. The DES is actually a cube, but its thickness is 200μ, which is small enough compared to the others in this formula to be ignored.

Electrode materials, electrode attachment methods, elastomer improvements, electrical circuits, etc. are being developed as DE/DES components. In order to produce flexible electrodes, the materials used for them include metal foil (including liquid metal), carbon grease, carbon particles (e.g., carbon black), carbon nanotubes (CNT), and conductive polymers [4,39,40]. If a larger electrode deformation is required, it is better to use highly conductive CNTs (especially single-wall CNTs) [41]. Liquid metal or carbon grease is less suitable due to grease leakage. However, with good insulation, leaks are less likely to occur, but this imposes some restrictions on operation [4]. M. Han et al. proposed a pressure sensor composed of a CNT-polydimethylsiloxane (CNT-PDMS) composite electrode and a porous polymer dielectric layer as a medical wearable sensor [42]. While the concept is interesting, this wearable sensor might not work well because the electrodes are not flexible enough and the polymers used are stiff. Carbon black and several different polydimethylsiloxanes (PDMS) have been studied on electrode compositions also [43]. It used a change in resistance rather than a change in permittivity. However, using a device (a C/V converter) that can be measure even a small capacitance, a DES enables measurements of pressure at even smaller deformations [40]. Electrodes can be made by dissolving CNT or carbon black in a solvent, mixing in a small amount of binder, and applying it to the elastomer with a brush or paint [22,44]. H. Shigenune et al. applied the CNT ink using a finger or a slightly larger brush, which left traces of the brush or finger on the surface of the electrode, unfortunately resulting in uneven thickness of the electrode [44]. M. Amjadi et al., although not DE, dispersed a Multi-wall CNT (MWCNT) in a silicone elastomer and created a sensor using the change in resistance [45]. However, after spraying, it was annealed to increase the strength of the film. As a result, the film would be stiffened and have limited elongation.

C. Walker et al. used five layers of sensors to detect the position of a robot fish fin [46]. S. Chiba et al. prepared a softer material by adjusting the dangling chains of the elastomer and the cross-linking agent, and created a sheet-type pressure DES, demonstrating their usefulness [39]. G. Rizzello also points out the usefulness of DESs made of thin layers of soft dielectric materials (acrylic, silicon,

 doi:10.20944/preprints202307.0181.v1

etc.) [47]. Venemann et al. used a softer commercial acrylonitrile-butadiene rubber (NBR) containing a large amount of plasticizer as the base material for the dielectric layer of the DE [48].

As an example of circuit research, K. Jung et al. used a system that mixes a low-frequency signal for operation with a high-frequency signal of small amplitude for detection to realize DEA drive and motion detection using modulation techniques. [49]. H. Bose et al. conducted an experiment using a thicker mat-type pressure sensor instead of a sheet-type DE [50]. They also considered making the DES structure a waveform and making it into an array. Unfortunately, however, the size of the sensor is larger than that of the sheet type, and the material is silicon, so it might not be able to expand much, which might limit its application [51]. S. Seelecke et al. proposed side-by-side silicon-based diaphragm-type DEs to enable cooperative sensing and tactile functions [52]. Regrettably, silicon has low elongation, and the diaphragm-type DE array type is a fixed-point measurement type sensor similar to a sensor that measures resistance. It could therefore be difficult to accurately follow the movement of limbs and measure them [39].

Finally, as an example of a possible application, R. Walker et al. carried out a study in which DES was attached to a diver's wetsuit and movement was monitored. [53]. C. Larson et al. placed a large number of DES on the body of a game player and attempt to apply it to a virtual reality game in which the game can be played by moving the body [54]. As another example of system research, it was pointed out that the DEA/DES system, which combines DES and DEA, could assist in the movement of patients' fingers, hands, feet, etc., and could possibly be used to accurately evaluate the progress of physical rehabilitation [55]. R. Venkatraman et al. attempted to measure blood pressure using a DE cuff device [56].

It is highly possible that the DE could be used simultaneously as an actuator and pressure and/or position sensor [57]. In the very near future, it might also become possible to create intelligent robot limbs and nursing care equipment using DEAs/DESs, which would assist the movement of a patient's fingers, hands, feet, and so on. Furthermore, this technology could possibly evaluate the rehabilitation status with great accuracy [58]. However, developing such devices will require further improvements in DEA/DES performance. The main factors for this are the improvement of the conductivity of the electrode and its flexibility, and the flexibility of the elastomer should also be sufficiently improved [41,59].

3. Experimental procedure

The purpose of this experiment is the following two points.

(1) A stretch DES and a pressure DES, which are made by combining SWCNT electrodes with greater stretchability and flexibility and a film with improved hardness and elongation of HNBR, are attached to robot's finger, and the motion of the finger is sensed, and the force (pressure) when the finger touches the object is detected.

(2) In addition, assuming the use of a virtual system or the like, in order to drive the robot's finger as the human operator wishes, stretch sensors are attached to the fingers of the human and the robot, and a system is constructed to transmit the movement of the fingers from the human to the robot. Thus, a system by replacing human finger movements with robot fingers can be demonstrated. An additional experiment was conducted in which a vibrator using a small DEA was attached to the fingertip of the robot, and the sensation of contact with the object was transmitted to the human finger.

3.1. Adjustment of elongation (hardness) and film formation of hydrogenated nitrile rubber (HNBR)

HNBR (prepared by ZEON Corporation) is a material that is laid under the car engine to absorb the vibration of the engine. HNBR can be used in relatively hot environments and has excellent heat resistance, oil resistance, dielectric strength, and a high dielectric constant. [57]. Therefore, in the near future, HNBR is expected to be utilized in a high-power DEAs or wave power generation. However,

Preprints (www.preprints.org) | NOT PEER-REVIEWED | Posted: 4 July 2023 doi:10.20944/preprints202307.0181.v1

it is now used to absorb engine vibrations, so it is stiff and not suitable for DEs. An attempt has been made to improve the elongation (hardness) by adjusting the amount of the cross-linking agent added and cutting some of the double bonds (see Figure 1). The following shows how to adjust the amount of cross-linking added and how to cut a part of the double bond:

1) How to adjust crosslinking agents:

HNBRs were dissolved in MEK (methyl ethyl ketone), organic peroxide (1,3 1,4-bis (t-butylperoxyisopropyl benzene)) was added, and it was mixed with a dispersion machine. Next, it was dried naturally to remove the solvent and obtain a mixture. Finally, the mixture was pressed at 150 ° C and made into a film.

2) Dangling bond reduction method:

By reducing the double bond of the HNBR, the generation of dangling bonds caused by oxidative deterioration, or other processes, originating from the double bond was reduced. In other words, by improving the hydrogenation rate (crushing the double bond with hydrogen), both the generation of double bonds and the organic peroxide as the starting point was eliminated as much as possible, which eliminated the double bonds as much as possible.

After carefully hand-casting the HNBR film, 4 locations on the film were selected and the film thickness was checked to make sure that the film thickness was uniformly 200 μm, using a digital thickness gauge (SMD-565A-565A-565A) by TECLOCK Co., Ltd.

3.2. Tensile test

A tensile test of the dumbbell-shaped test piece (see Figure 3b) was performed using the Orientech tabletop material tester STA-1150 (see Figure 3a). The displacement velocity was set to 500 mm / min.

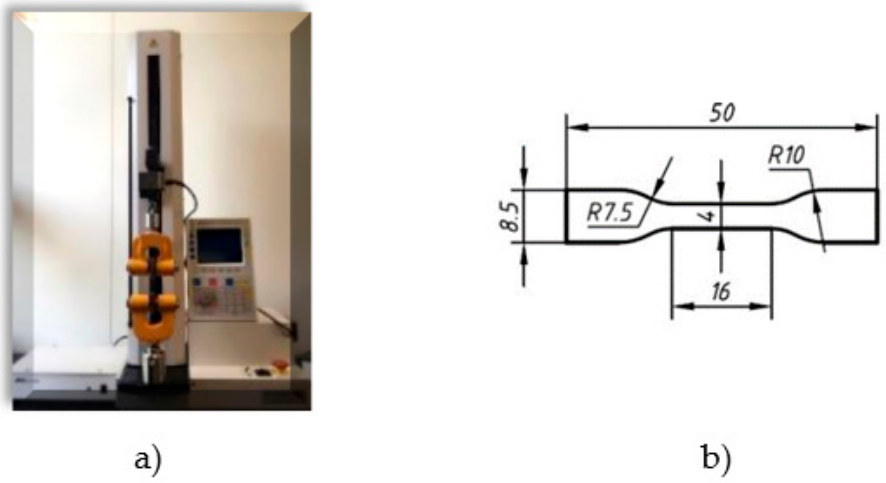

Figure 3. Desktop material tester (Orientech STA-1150) shown in a) and the dumbbell-shaped test piece shown in b).

3.3. Electrode materials for DES and their adhesion method

SWCNT (Zeon corp. ZEONANO®-SG10) was selected as a highly conductive material that can be molded into a compliant electrode. A sprayable CNT solution was developed to facilitate electrode fabrication. It was prepared by mixing dispersed CNTs and a binder. For the CNT dispersion, CNT and 2 wt% sodium cholate were first added to the dispersion medium and dispersed using an ultrasonic homogenizer [41]. This solution was placed in a spray can and used as a spray (see Figure 4). Figure. 4a shows a scene of making a thin film electrode by spraying. The continuity test is also shown in Figure 4b. Figure 5 shows a container containing spray, dispersed CNTs and a container containing solvent. When spraying, insert a container containing CNTs is inserted into the side of the spray nozzle and used (see Figure 4a). In addition, it is better to clean the nozzle after use, so it is recommended to insert the spray nozzle into a container with cleaning solvent and clean it. After

Preprints (www.preprints.org) | NOT PEER-REVIEWED | Posted: 4 July 2023 doi:10.20944/preprints202307.0181.v1

creating the SWCNT electrode film on the elastomer, several locations were randomly selected and the thickness was measured with a Keyence double scan high-precision laser measuring instrument (LT-9500 & LT-9010M), all of which were 50 μm. In addition, in order to confirm the degree of dispersion of the SWCNTs, SWCNTs before and after dispersion were confirmed by SEM.

To confirm that the SWCNTs were uniformly sprayed onto the elastomer surface, four points on the surface of the DE sample were arbitrarily selected and observed using SEM.

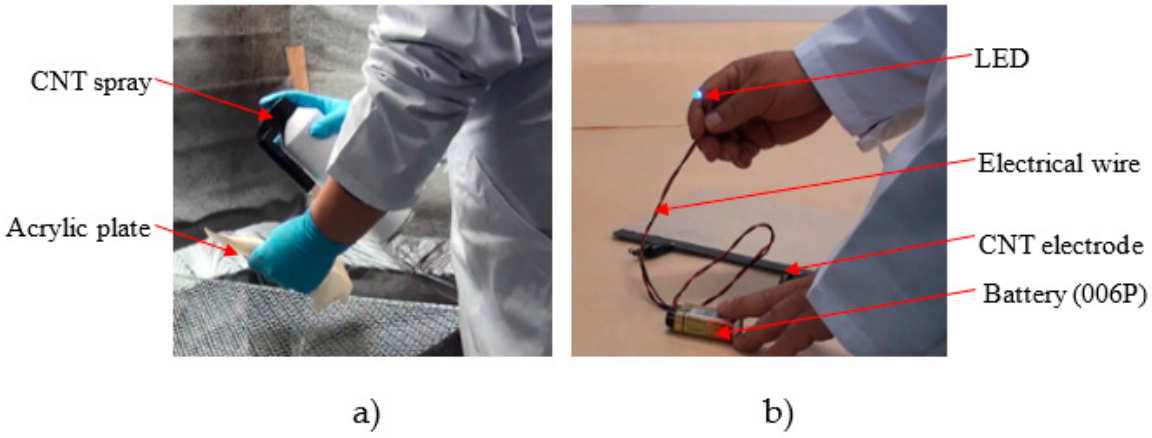

Figure 4. Using SWCNT spray to generate electrodes on the object (Fig. 4a) and the continuity test (Fig. 4b): a) SWCNTs being sprayed on objects; b) After spraying, test operation with LED and battery.

The membrane size used was 20mm (diameter) for the pressure sensor and 10 mm x 20 mm for the stretch sensor. Both film thicknesses were 200 μm.

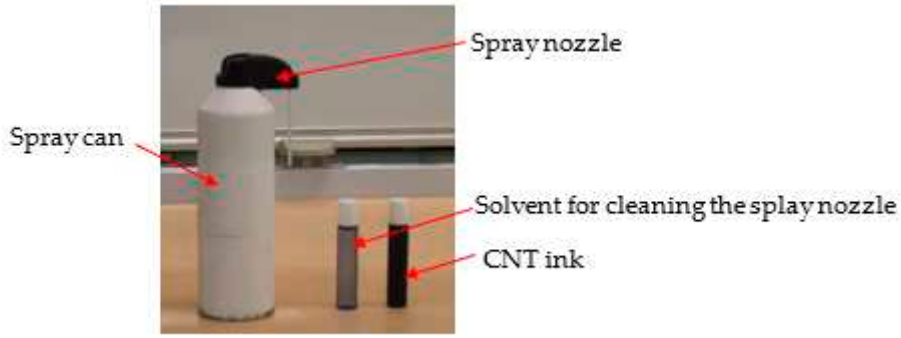

Figure 5. A SWCNT spray set.

3.4. Measuring capability of pressure DES

The change in capacitance due to deformation of the pressure DES prepared by the above method was measured using an NF LCR METER (ZM2372).

3.4.1. Overview of the pressure DES used in this experiment

Figure 6 shows the prototype pressure DES using HNBR ver.6. This pressure DES has a diameter of 20 mm and uses the Ver.6 with a thickness of 200μm as the main material. Electrodes were created using the CNT spray introduced above. The Ver.6 is extremely soft, so, by attaching this to a sheet (supporting material) made of H05-100J manufactured by Exeal Co., Ltd., a structure can be deformed even with a small load. The H05-100J urethane material used here has a hardness of Asker C0/7, which is relatively soft.

Preprints (www.preprints.org) | NOT PEER-REVIEWED | Posted: 4 July 2023 doi:10.20944/preprints202307.0181.v1

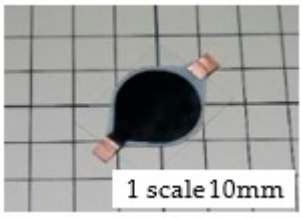

Figure 6. The prototype of a pressure DES using HNBR.

3.4.2. Overview of the experimental system

Figure 7 is the test bench for the pressure DES. A micrometer was attached to the XYZ axis precision stage, and a load was applied from above the pressure DES to deform it and measure it. The pressure DES used in the experiment was attached to the top of the load cell installed on the XYZ axis precision stage. Two load cells with maximum measurement loads of 2 kg and 10 kg were used for measurement due to the measurement range. The analog signal output from the load cell was input to the microcomputer (ATmega328) via a dedicated AD conversion IC (HX711). After that, calibration processing was performed by the microcomputer, and the measured valkonnba-taues were displayed on the LCD. For the load measurement accuracy, it was confirmed that the error was 5% or less using a weight whose mass had been measured in advance.

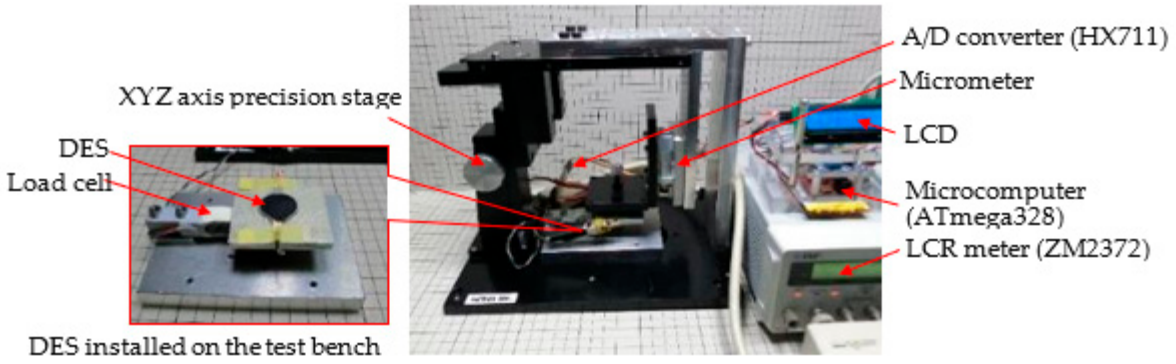

Figure 7. Overview of the test bench used for the pressure DES experiment.

3.5. Measurement of stretch ability of stretch DES

Outlines of the stretch DES used in the experiment and the experiment system are described as follows:

3.5.1. Overview of the stretch DES used in the experiment

Figure 8 shows the prototype of the stretch DES using HNBR ver.6. The basic configuration is the same as the pressure DES described in Section 3.4. However, in consideration of attaching it to a robot hand, the shape is a rectangle of 10 mm in length and 20 mm in width, and no support material is used.

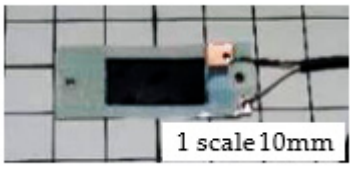

Figure 8. The prototype stretch DES.

3.5.2. Overview of the stretch DES system for the experiment and experimental method

Preprints (www.preprints.org) | NOT PEER-REVIEWED | Posted: 4 July 2023 doi:10.20944/preprints202307.0181.v1

The test bench for the stretch DES has a structure in which the movable part moves between the linear slides attached to the fixed part. A stretch DES can be stretched by fixing both ends to a fixed part and a movable part and rotating the ball screw. The stretched length was measured with digital calipers attached to the fixed and movable parts, and the capacitance was measured using an LCR meter (ZM2372) manufactured by NF Corporation. Figure 9 shows the prototype of the stretch DES using HNBR ver.6. Figure 10 shows the test bench for the stretch DES.

The method for measuring capacitance is shown as follows. The unstretched length of the stretch DES was set to 0 mm (see Figure 23a). From that point it was stretched to 80 mm (Figure 23b) and the capacitance was measured.

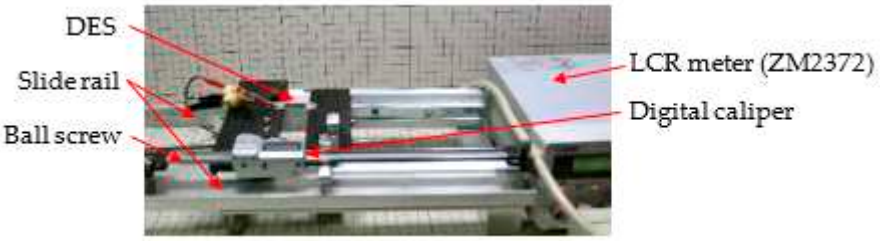

Figure 9. The test bench for the stretch DES.

3.6. Measurement of DES response speed

The response speed of the DES pressure sensor was verified by measuring the time from when the capacitance started to change when a sudden load was applied to the DES pressure sensor until it stabilized. The DES pressure sensor used in the experiment has the same specifications as in Section 3.4. A weight of 10g was dropped from a height of 10mm onto the DES pressure sensor mounted on the aluminum plate, and the change in the detected capacitance was converted into a voltage by the detection circuit. In the case of stretch DES, the response speed of the DES was verified by measuring the time from when the DES was stretched (or pressured) on the test bench to when the capacitance started to change. The DES sensor used in the experiment has the same specifications as in Section 3.5. The stretch DES was stretched by a stepper motor attached to the test bench. In addition, the extension start timing was detected by a 3-axis acceleration sensor (ADXL-345 manufactured by ANALOG DEVICES Inc.) attached to the test bench.

The change in DES capacitance is converted to voltage by the detection circuit, and measured along with the decompression start timing via a 16-bit A/D conversion IC (ADS1115) made by TEXAS INSTRUMENTS and a microcomputer (ATmega328P) made by Atmel. Figure 10 shows how the DES response speed is measured.

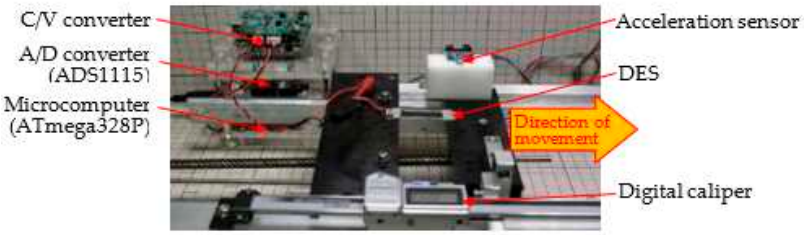

Figure 10. Measuring the response speed of a DES.

As with the stretch sensor, changes in DES capacitance were converted to voltage by a detection circuit and measured via a 16-bit A/D conversion IC (ADS1115) made by Texas Instruments and a microcomputer (ATmega328P) made by Atmel.

3.7. Measurement of robot finger movement and finger pressure, and an experiment to transmit the sensation of the robot finger touching an object to a human finger

Preprints (www.preprints.org) | NOT PEER-REVIEWED | Posted: 4 July 2023 doi:10.20944/preprints202307.0181.v1

First, the motion of the robot's finger was sensed using a stretch DES, and the force (pressure) when the fingertip touched the object was measured. Figure 11 shows the stretch DESs and pressure DESs attached to the robot hand.

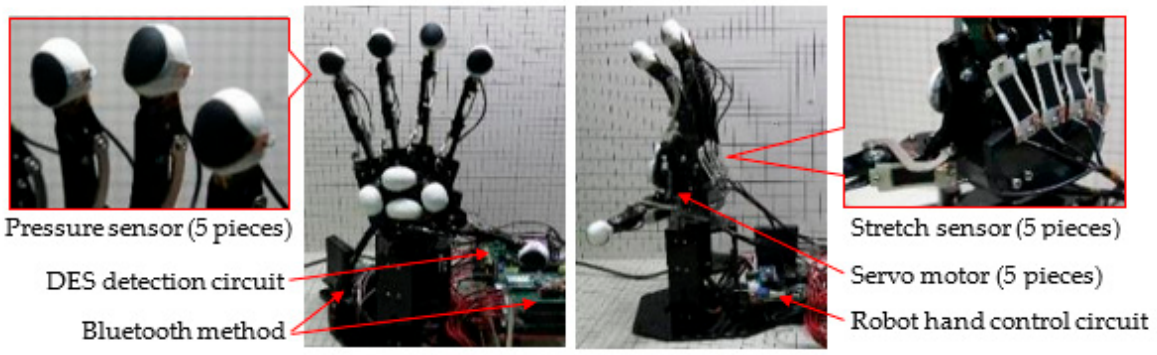

Figure 11. The stretch DESs and pressure DESs attached to the robot hand.

Five pressure sensors were used and attached to the tip of each finger. The shape of the pressure sensor was a circle with a diameter of 20 mm. The stretch sensor was a rectangle of 20 mm in length and 10 mm in width. Five stretch sensors were attached to the base of each finger. The detection circuit of each sensor was placed on the back of the hand to shorten the analog signal wiring and prevent malfunction. Five model micro servo motors (product model number: MG90S) with a maximum torque of 2.2 kg/cm and a weight of 13 g were used to drive the fingers. Figure 12 shows a block diagram of the drive system and sensing circuit of the robot hand.

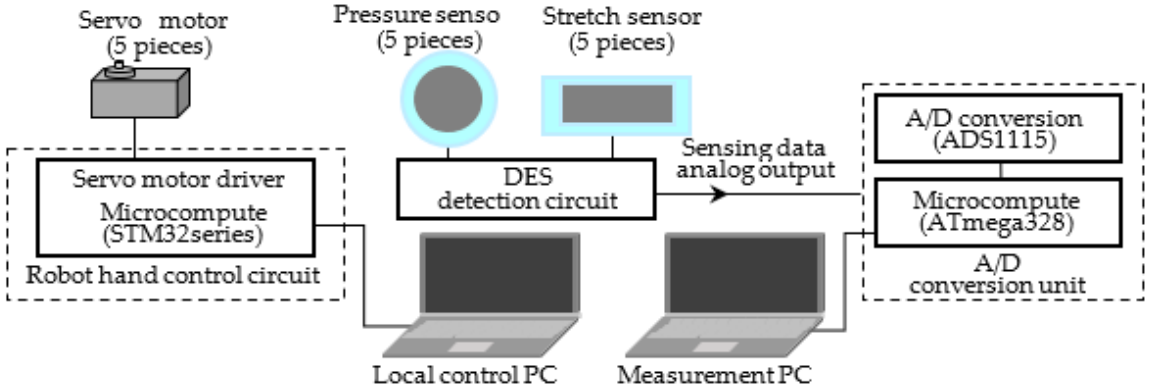

Figure 12. Block diagram of the drive system and sensing circuit of the robot hand.

A microcomputer (STM32 series) manufactured by STMicroelectronics was used to drive the robot hand. Also, by connecting the microcomputer and the local control PC with a USB cable, it can be moved like a human hand. A pressure sensor and a stretch sensor are attached to each finger. The signals detected by these sensors were converted to analog signals by the detection unit, converted to digital signals by the A/D conversion unit, and then recorded by the measurement PC. The A/D conversion unit used for the measurement consists of a 16-bit A/D conversion IC (ADS1115) manufactured by TEXAS INSTRUMENTS and a microcomputer (ATmega328P) manufactured by Atmel (see Figure 13).

Figure 13 shows a driving experiment of a robot hand equipped with the pressure sensor and the stretch sensor. Using this system, the detection status of the pressure sensor and stretch sensor was confirmed by holding the ball with the thumb and index finger.

Preprints (www.preprints.org) | NOT PEER-REVIEWED | Posted: 4 July 2023 doi:10.20944/preprints202307.0181.v1

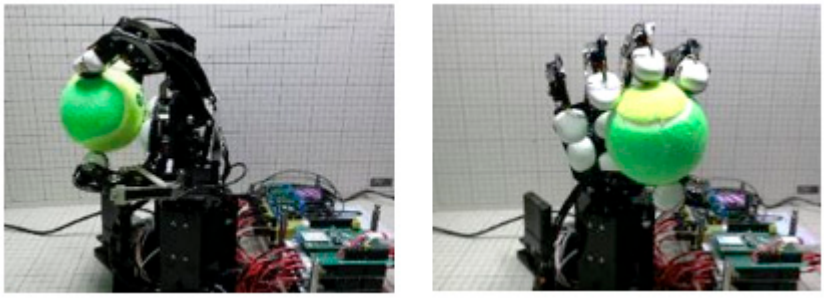

Figure 13. State of driving experiment of robot hand.

By bending the index finger of the robot hand, it was confirmed that the detection signal of the stretch sensor increases. Also, it was confirmed that the pressure sensor responds when the tip of the index finger touches the ball. In addition, an experiment was also conducted to transfer human finger movements to robot fingers. Furthermore, an experiment was conducted in which a small diaphragm-type vibration DEA (active part diameter: 6 mm) [60] was applied to a human finger to feed back the sensation of the robot finger touching an object to the human finger. Figure 14 shows how a small diaphragm-type vibration DEA is attached to a human hand. Figure 14a is a small diaphragm-type vibrating DEA. The donut-shaped black parts are the electrodes, which are placed in front and back with the elastomer sandwiched between them. Figure 14b shows a small diaphragm-type vibration DEA unit mounted in a control sensor glove. The brown part is insulating tape made of polyimide. Fingers and the DEA are held in the glove by acrylic DEA folders.

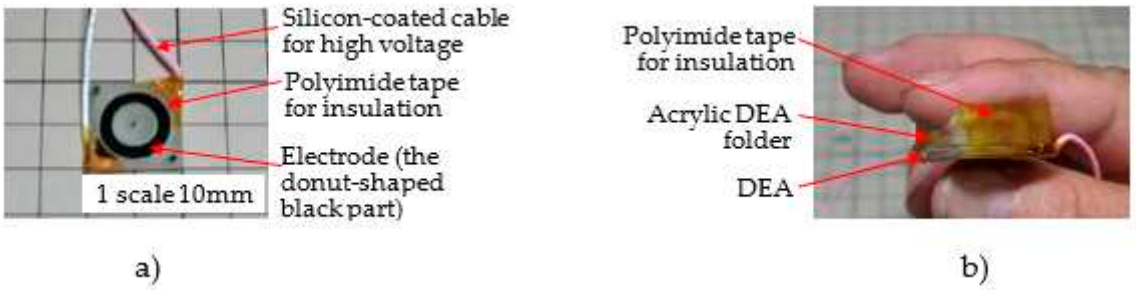

Figure 14. Attaching a small diaphragm-type vibration DEA to the fingertip: a) a small diaphragm-type vibration DEA; b) the DEA attached to a human finger.

The DEA had an outer diameter of 6 mm, and the elastomer used was 3M4905. Electrodes were made by spraying SWCNTs (see Figure 6) [60]. As mentioned above in how to make a pressure DES, the reason why HNBR ver.6 was not used for this vibrator DE is that the Ver.6 is too soft for the DE.

Next, Figure 15 shows a block diagram of the driving system and sensing circuit of the robot hand, the sensor glove, and the small diaphragm DEA driving system.

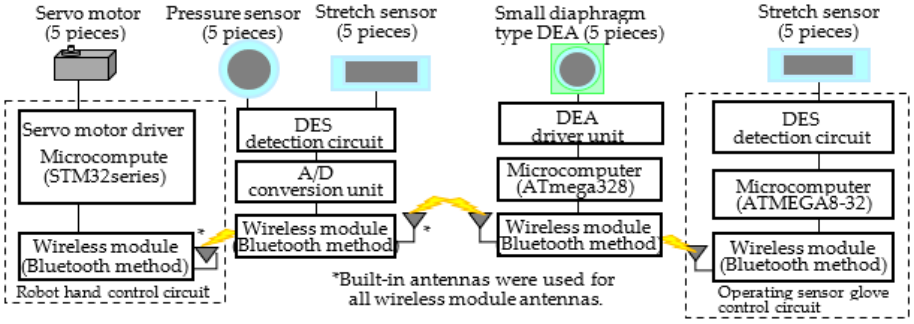

Figure 15. Block diagram of the drive system and sensing circuit of the robot hand, the operating sensor glove, and the small diaphragm type DEA drive system.

Preprints (www.preprints.org) | NOT PEER-REVIEWED | Posted: 4 July 2023 doi:10.20944/preprints202307.0181.v1

The drive system and sensing circuit of the robot hand are almost the same as those shown in Figure 13 above, but the following points have been changed in order to connect the operating sensor glove and the small diaphragm DEA drive system.

The first change is that in Figure 12, the servo motor drive signal was supplied from the local control PC, but in this system, the servo motor drive signal is supplied from the operation sensor glove via the wireless module. This makes it possible to remotely control the robot hand from several meters away. The second change is that the signal detected by the pressure sensor is used as the drive signal for the small diaphragm DEA. In this system, the analog signal detected by the pressure sensor is converted into a digital signal by the microcomputer (ATmega328) installed in the A/D converter unit, and supplied to the drive system of the small diaphragm DEA via the wireless module. Next, an overview of the operation of the operation sensor glove and the drive system of the small diaphragm DEA will be described. A finger movement is detected as a change in capacitance by a stretch sensor attached to the operation sensor glove. The detected change in capacitance is converted to an analog signal by the DES detection circuit and supplied to an Atmel microcomputer (ATmega8-32). The drive signal for the small diaphragm DEA is generated by a microcomputer (ATmega328) based on the pressure signal supplied from the robot hand, adjusted to an appropriate voltage by the DEA driver, and then supplied to the small diaphragm DEA. Figure 16 shows how the prototype robot hand is controlled by the operation sensor glove.

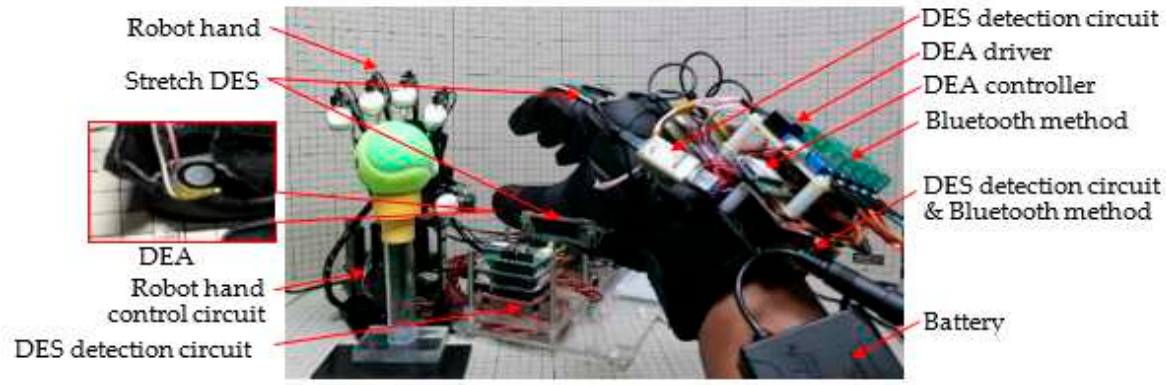

Figure 16. Prototype robot hand and operation sensor glove.

4. Experimental results

The results of the experiments described in the experimental methods above are shown below.

4.1. Adjustment of HNBR additives and reduction of dangling bonds

Table 1 shows the results of the adjustment of HNBR additives and reduction of dangling bonds.

Table 1. Adjusting HNBR additives and reducing dangling bonds.

	Crosslinking agent (when rubber is 100)	Crosslinking agent name	Crosslinker (molecular weight)	Double bond amount (%)
HNBR original film	8	1,3 1,4-bis (t-butyl alcohol isopropyl alcohol) Benzene	338.5	10
HNBR film ver.1	8	Same as above	338.5	5
HNBR film ver.3	2	Same as above	338.5	1

Preprints (www.preprints.org) | NOT PEER-REVIEWED | Posted: 4 July 2023 doi:10.20944/preprints202307.0181.v1

HNBR film ver.6	1	Same as above	338.5	1

In the previous experiment, Ver.3 was used, and the measurable pressure ranged from 4kgf to 120kgf [39]. However, this time, this experiment was conducted using the softer Ver.6 in order to be able to measure lower pressures.

4.2. Results of the tensile tests

Figure 17 shows the results of a tensile test using HNBR with adjusted additives and reduced dangling bonds.

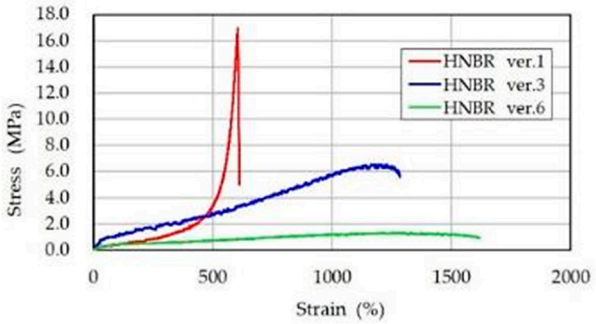

Figure 17. HNBR tensile test results.

Compared to the original HNBR (before the improvement), when looking at Ver.3 and Ver.6, it can be seen that the growth has increased sufficiently in Ver.6.

4.3. Confirmation of the degree of dispersion of SWCNTs and Confirmation of the electrode surface with SWCNTs sprayed on elastomer

The SWCNTs were well dispersed to create a SWCNT spray. Figure 18 shows SEM photographs before and after dispersion. As shown in Figure 18, it can be seen that they are sufficiently dispersed.

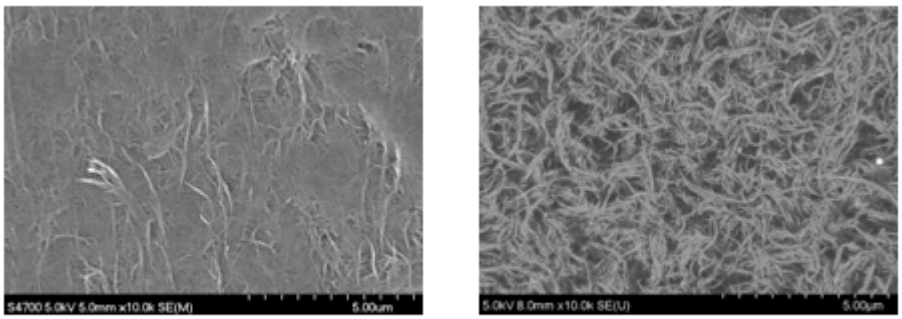

a) b)

Figure 18. SWCNTs before and after dispersion (magnification: X10,000): a) SWCNT before dispersion; b) SWCNTs after dispersion.

To confirm that the SWCNTs were uniformly sprayed onto the elastomer surface, four points on the surface of the DE sample were arbitrarily selected and observed using SEM. As a result, as shown in Figure19, it can be seen that the SWCNTs are uniformly sprayed.

Preprints (www.preprints.org) | NOT PEER-REVIEWED | Posted: 4 July 2023 doi:10.20944/preprints202307.0181.v1

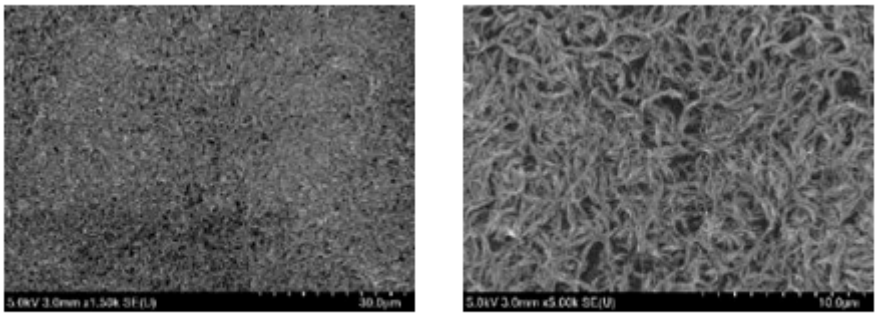

a) b)

Figure 19. Electrode surface by spraying SWCNTs: a) Magnification: X1,500; b) Magnification: X5,000).

4.4. Measurement results of the pressure DES

For the measurement, the length of the micrometer attached to the XYZ-axis precision stage was adjusted to increase the load applied to the DES pressure sensor, and the capacitance at each load was measured. As shown in 3.4.2 above, since the measurement range of the load cell used this time is narrower than the measurement range of the DES pressure sensor, the measurement range was divided into two times, 1gf to 2kgf and 2kgf to 20kgf. Figure 20 shows the capacitance when each load is applied.

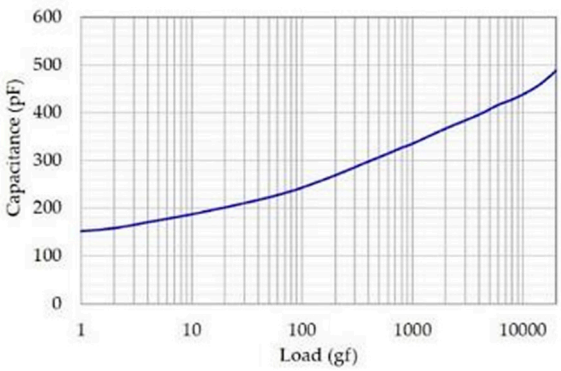

Figure 20. The capacitance when a load of 1gf to 20kgf is applied.

The capacitance changes almost linearly from 1g to the measurement limit of 20kg.

4.5. Measurements of DESs' response speeds

Figure 21 shows the change in the measured stretch DES capacitance. A is the point where the DES displacement begins, and B is the point where the capacitance begins to change. The time from point A to point B was 50ms, and it was confirmed that sufficient driving speed was obtained for use in a robot hand. Thus, the response speed of the stretch DES was 50ms.

In the case of pressure DES, according to the measurement method in section 3.6 above, the speed of the pressure was measured and it was 50ms. That is also fast enough.

Preprints (www.preprints.org) | NOT PEER-REVIEWED | Posted: 4 July 2023 doi:10.20944/preprints202307.0181.v1

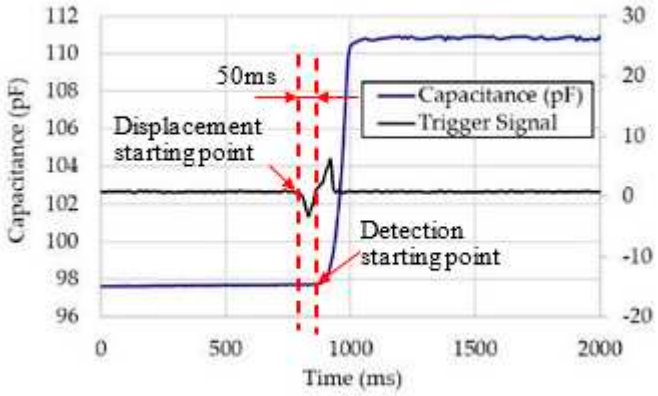

Figure 21. Changes in measured capacitance.

4.6. DES stretching ability measurement results

Figure 22 shows the changes in capacitance when the DES stretch sensor is stretched. As shown in the section of 3.5.2, the method for measuring capacitance, the unstretched length of the stretch DES was set to 0 mm (see Figure 23a). From that point it was stretched to 80 mm (Figure 23b) and the capacitance was measured. Since the length of the sensor part of the stretch DES is 20 mm (see Figure 8), it was confirmed that the sensor can be stretched by 400% (See Figure 23). It can be seen that even with a slight elongation of about 10%, the capacitance changes, and even with an elongation of more than 400%, the capacitance changes almost linearly. Figure 23 shows a photograph of the stretch DES stretched over 400%. Even after being stretched over 400%, it still remains conductive and it can be seen that sensing is possible.

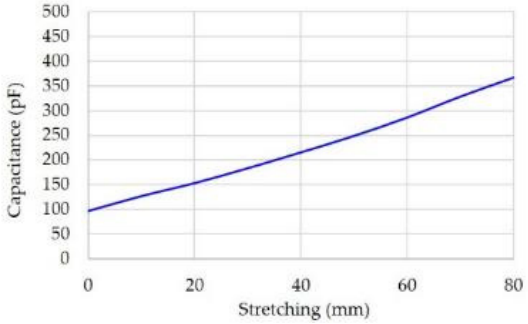

Figure 22. A graph showing changes in capacitance when the stretch DES is stretched.

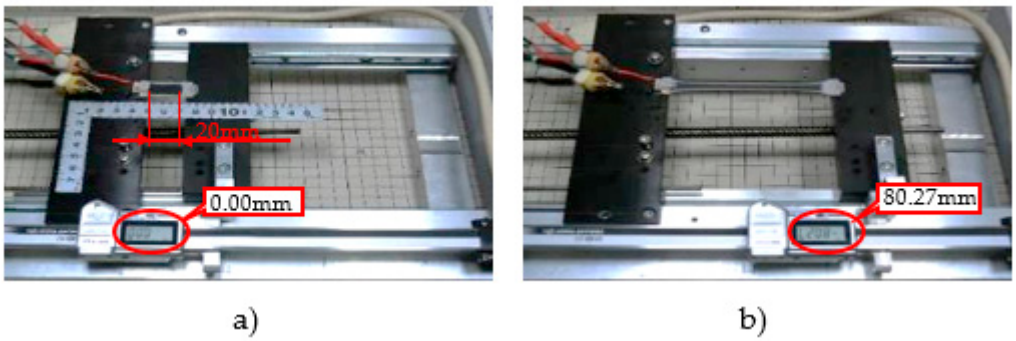

Figure 23. Photographs of the stretch DES stretched over 400%: a) before stretching; b) after stretching.

Preprints (www.preprints.org) | NOT PEER-REVIEWED | Posted: 4 July 2023 doi:10.20944/preprints202307.0181.v1

Changes in capacitance with an LCR meter while stretching were measured. The elongation was measured using a digital caliper, and the lengths were compared. In both cases, an electric current was applied to check the conductivity, and the LED was turned on.

4.7. Measurement result of the pressure felt by the finger of the robot using the pressure DES and the result of the experiment that conveys the feeling of the robot finger touching an object to the human finger using the small diaphragm type vibrator DEA.

Using a robot hand drive system equipped with a pressure sensor and a stretch sensor, the detection status of the pressure sensor and stretch sensor was confirmed by holding the ball with the thumb and forefinger. Figure 24 shows transitions of analog signals of fingertip pressure and finger displacement detected by the pressure sensor and the stretch sensor at this time.

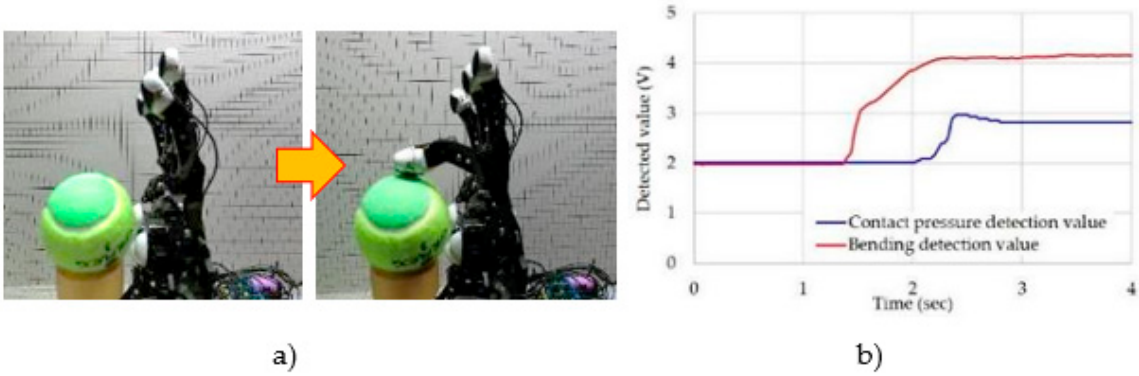

Figure 24. The fingertip pressure and finger displacement detected by the pressure sensor and stretch sensor attached to the index finger of the robot hand: a) Movement to hold the ball with the thumb and index finger); b) Transitions of the analog signals of fingertip pressure and finger displacement detected by the pressure sensor and the stretch sensor.

Figure 25 shows the robot hand being operated by the sensor glove worn on the hand. It was confirmed that the same movements as the hand can be reproduced with the robot hand.

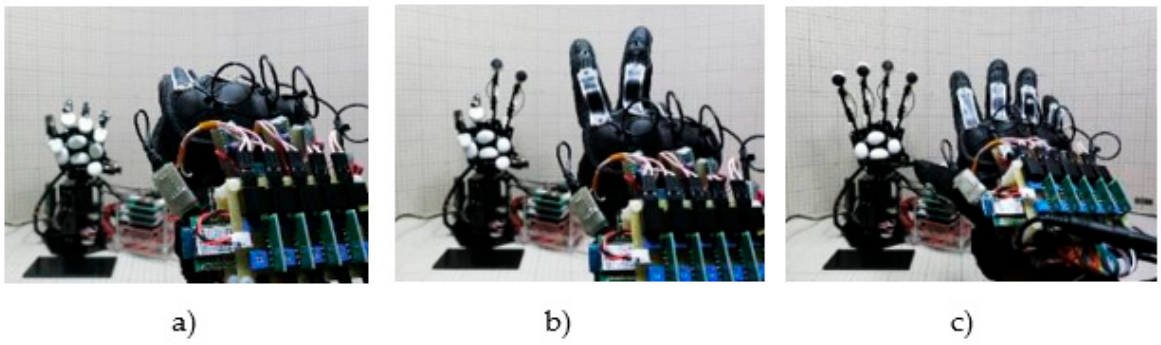

Figure 25. Manipulation of the robotic hand using the manipulator sensor glove: a) grasping using all fingers, b) opening index and middle fingers and c) opening all fingers.

5. Discussion

As mentioned above, the pressures that can be measured up to now range from about 5kgf to about 120kgf, and pressures lower than about 5kgf could not be measured [39]. However, this time it became possible to measure from 1gf to 20kgf (see Figure 20). A major factor behind this is that the yield point stress values of 3M acrylic film (4905) and HNBR ver.6 are about half or less (see Figure 26). In other words, even if a little pressure is applied, the film can be deformed, and the slight change in capacitance can be measured.

Preprints (www.preprints.org) | NOT PEER-REVIEWED | Posted: 4 July 2023 doi:10.20944/preprints202307.0181.v1

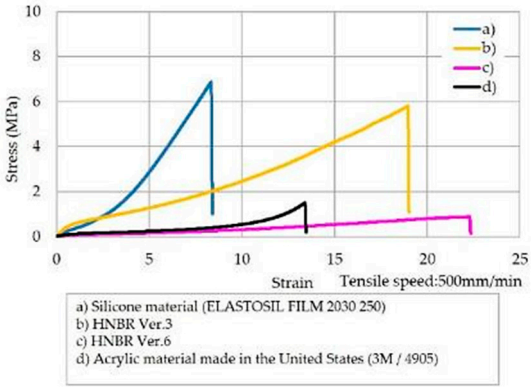

Figure 26. The results of the SS curves of the silicon (ELASTOSIL FILM 2030 250: shown in blue), the acrylic material made in the United States (3M / 4905: shown in black), and the HNBR (ver.3: shown in orange and ver.6: shown in pink).

This HNBR pressure DES can measure any pressure anywhere within the measuring range. As mentioned above, the reason for this is that Ver.6 has been softened, and another point is that it depends on the circuit design (see Chapter 3.4). Circuits with higher amplification can also be used to measure smaller changes, thus increasing the measurement range. In other words, the pressure measurement range of the DES changes depending on the hardness of the material used, the shape of the sensor, the tune-up of the detection circuit, etc., so it is important to select those specifications according to the purpose [39]. From those results, it is possible to improve their performance. Incidentally, in this experiment, the response speed of this DES was 50ms. This response speed, like pressure measurement, also depends on the hardness of the film and the circuit.

Table 2 shows the response speed of the pressure sensor for different elastomer types and electrode types [39]. As shown in Figure 26, it can be seen that the silicon material is harder than other films, and as seen in Table 2, it has a fast response speed as a sensor. However, due to its small elongation, its application is considered to be limited. In other words, materials with low dynamic viscoelasticity, such as silicon, are not suitable DEA/sensor materials [39]. On the other hand, acrylic and HNBR are softer and more elastic than other films, making them suitable materials for sensors. The response speed is also sufficient for practical use, and it seems to be optimal as a sensor that is used in close contact with a person's finger.

Table 2. Difference in response speed when changing the type of elastomer and electrode.

	Carbon grease	Carbon black	SWCNT
Silicone material (ELASTOSIL FILM 2030 250)	69	66	59
HNBR Ver.3	80	78	68
Acrylic material made in the United States (3M / 4905)	93	86	73
The film that corrected the distortion of the 3M/4905 acrylic	94	88	74

Note: Each of the above measurement data was confirmed in the load cell. The unit of speed is milliseconds.

It was found that the capacitance of this stretch sensor changes even when it is stretched by only about 10%, and the capacitance changes almost linearly even after it was even stretched by more than 400% (see Figure 22). Also, the speed of stretch DES was 50ms. In this experiment, the stretch DES was attached to a human glove in close contact. As a result, the sensor responded to the bending motion of the glove (fingers), and the motion could be transmitted to the robot quickly in a synchronized state. In other words, it seems that this sensor speed was fully sufficient. A stretch DES, like a pressure DES, also depends on the stiffness of the membrane. In the case of the circuit, as

 doi:10.20944/preprints202307.0181.v1

mentioned again, using a higher amplification circuit allows smaller changes to be measured, increasing the measurement range. Thus, the elongation of this sensor depends on hardness, as it does with pressure.

It was also confirmed that the feeling of the robot fingertip touching the ball was obtained from the small diaphragm DEA attached to the operation sensor glove for a human operator (see Figure 25). In this prototype system, four microcomputers and four wireless modules are used to construct the system, but by reviewing the circuit, it is thought that the number of these used can be reduced to about half. Also, since the wireless module used this time uses the Bluetooth method, the operation range was several meters, but by changing the wireless module to the Wi-Fi method, the operation range can be extended to several tens of meters. From these matters, it has become possible to move the robot's finger in real time in accordance with the movement of a human.

Furthermore, if the Internet is available, it can be operated from anywhere in the world. The use of 5G and 6G technology, which has been expanding in its use, will enable low-latency operation, so it can be applied to fields such as telemedicine that require precise operation. HNBR Ver.6 at this time is not suitable for DEAs because the adjustment method of the amount of cross-linking agent and the adjustment of dangling bonds were altered considerably, so the hardness was considerably reduced, so the strength of the film was low. Therefore, 3M/4905 was used in this experiment.

Moreover, if this stretch sensor has the capability to be used as a three-dimensional position sensor for the arms and legs of robots and the like. To explain step by step, first a stretch sensor would be attached to the upper side of the arm of the robot. When the arm is moved upward, the upper sensor is contracted, and the lower sensor is extended, so that it is possible to two-dimensionally determine at what angle the arm is bent. Furthermore, if another pair of sensors are arranged on the side of the arm, sensing diagonal movement is also possible. That is, the three-dimensional position can be easily determined from the difference in dielectric constant between the top and bottom and the difference in dielectric constant between the sides. Therefore, it is beneficial to prepare such a calculation table in the microchip.

It is expected that robots will work together with humans in the very near future, and it is necessary to match the movements of humans, so humanoid robots are desired. However, as the frequency of contact with humans increases, there is a strong need for robots to be safe for humans. For example, when a robot's hand touches a person, an excellent sensor can instantly determine that it is a person and stop the robot's movement or sufficiently reduce its output.

With this human-robotic interaction system shown above, a physician can possibly use a virtual system to palpate a patient when the patient is at a remote location [61]. In addition, in the assembly of a machine, when performing a detailed and sensitive assembly, it might be possible for a robot to do such work alone someday, although it still requires a skilled human at present. Using this system and AI, a robot could be taught the movements for its hands and fingers. As another example, it will become possible to feel the sensations shaking a hand or hugging someone virtually. As a step to realize the above-mentioned goals, the points obtained in this experiment might be a guideline for making an AI robot that could move and make decisions like humans in the future.

In 2012, the authors developed a system for the rehabilitation of patients who could not move their fingers due to conditions such as cerebral infarction by setting a DES capable of measuring the stretch of the patients' fingers and measuring how much they can move their fingers [62]. However, the DES at that time was not able to obtain sufficient elongation, which made it difficult to measure. However, with the new system, sufficient elongation can be obtained, so it is thought that the measurement can be performed accurately. Also, during rehabilitation, it is necessary to move the patient's fingers with the external force, but the DEA so far has not been able to respond sufficiently due to the small output. If the above DEA system (mentioned in Background of Dielectric Elastomers) developed in 2021 could be used, it would be possible to realize such a rehabilitation system without any problems [23].

As an electrode material, compared to multi-walled CNTs (MWCNTs) and carbon black, SWCNTs are more conductive, allowing for thinner electrodes and greater stretchability [41]. In this

Preprints (www.preprints.org) | NOT PEER-REVIEWED | Posted: 4 July 2023 doi:10.20944/preprints202307.0181.v1

experiment, the SWCNTs were sufficiently dispersed (see Figure 18), so even if the SWCNTs were packed in the spray, they could be sprayed without clogging [64].

It is worth mentioning that the above spray can impart conductivity to various materials such as wooden boards, glass, epoxy, rubber bands, elastomers, and insulating sheets. As a result, it is also easy for electrodes to follow curved surfaces (see Figure 27). It also remains conductive when bent, stretched, and rubbed. In addition, it will not come off even if when bent, stretched, or rubbed. Moreover, in terms of temperature resistance, HNBR sensors with SWCNT electrodes may be used at temperatures above 200 °C [63].

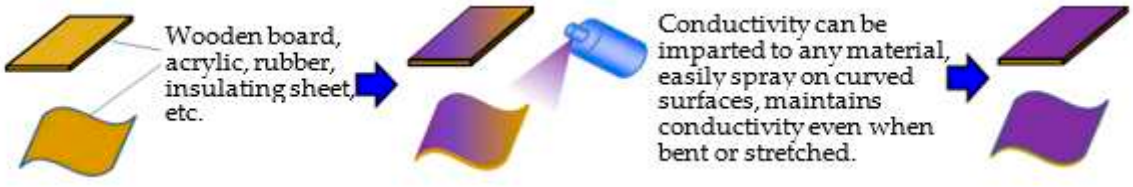

Figure 27. Image of forming electrodes by spraying SWCNT on various materials.

6. Conclusion

In this experiment, a DES that can measure low pressure, a stretch DES that can be greatly deformed, and a small diaphragm vibrating DEA were created. The following results were obtained by combining them.

- As a pressure DES was created using a very thin hydrogenated nitrile rubber (HNBR) film (0.2mm) with improved hardness and elongation. It enabled measurement at any pressure between 1gf and 20kgf.
- In addition, a stretch DEA with an elongation of 400% or more was developed using the same HNBR.
- Both a stretch DES and a pressure DES were attached to the finger of the robot, and the movement of the finger was sensed and the force (pressure) when the finger touched the object was also able to be detected.
- In order to drive the robot's fingers as the humans operator wished, a system was created in which the movements of the human fingers are transmitted to the robot's fingers by attaching the stretch sensors to the finger parts of the gloves made for humans and also to the robot's fingers. As a result, it became possible to move the robot's fingers following the human's movement.
- A vibrator using a small diaphragm DEA (the diameter of 6mm) was attached to the human fingertip so that when the robot finger touched the object, the sensation of the robot's fingertip was able to be transmitted to the human finger. As the result, it is now possible to add sensations artificially.

The results obtained from this experiment would hopefully serve as hints further promoting the development of robots that can be operated remotely by humans to perfectly reproduce the movements desired by humans, as well as the development of systems that can feed back the sensations of contact from robots. In addition, there is a strong demand for the realization of AI robots that can make more human-like movements and decisions using DEAs as the artificial muscles [22,23].

Acknowledgments: We would like to thank Mr. M. Uejima, Mr. H. Uchida and Mr. M. Takeshita of ZEON Corporation for providing SWCNT (ZEONANO® -SG101) and HNBR free of charge for carrying out our experiment.

References

1. Sarutani, T.; Takahashi, K.; Aga, T.; Yamagata, T. Small integrated pressure sensor, The Institute of Electronics, Information and Communication Engineering, Vol.J74-C2, No.5, pp. 333-339, May 25, 1991.
2. Shirakawa, H. Discovery of Conductive Polymers and Conductive Mechanism, Journal of Chemistry and Education, 67 (2), 82-85, 2019-02-20, (The Chemical Society of Japan), doi:10.20665/kakyoshi.67.2_82.

3. Harada, Y.; Suehara, T.; Ueno, T.; Higuchi, T. Development of an Actuator using Thermal Deformation, In Proceedings of the Spring Meeting of the Japan Society for Precision Engineering, pp. 803-804, the Japan Society for Precision Engineering, March 6, 2006, Tokyo, Japan, https://doi.org/10.11522/pscjspe.2006S0.803.0.
4. Zhang, L.; Gao, M.; Wang, R.; Deng, Z.; Gui, L. Stretchable Pressure sensor with Leakage-Free Liquid-Metal Electrodes, Sensors, 2019, 19, 1316, doi:3390/s19061316.
5. Ichinose, S. Current status and future of new materials for sensors, The Robotics Society of Japan, Vol.9, No.7, pp 883-887, 1991.
6. Ma, Z.; Li, S.; Wang, H.; Cheng, W.; Li, Y.; Pan, L.; Shi, Y. Advanced electronic skin devices for healthcare applications, Journal of Materials Chemistry B, vol. 7, no. 2, pp. 173–197, 2019, http://doi.org/10.1039/C8TB02862A.
7. Su, R.; Park, S.; Li, Z.; McAlpine, M. Robotic Systems and Autonomous Platforms, Advances in Materials and Manufacturing, Editors: Shawn M. Walsh, Michael S. Strano, pp. 547-557, Elsevier, 2019, ISBN: 9780081020487.
8. Al Moubayed, S.; Beskow, J.; Skantze,G.; Granström, B. A Back-Projected Human-Like Robot Head for Multiparty Human-Machine Interaction, Cognitive Behavioural Systems, In proceedings of the 2011 International Conference on Cognitive Behaviour Systems, pp. 114-130, Dresden, Germany, February 21-26, 2011.
9. Ponraj, G.; Kirthika, S.; Thakor, N.; Yeow, C.; Kukreja.; Ren, H. Development of flexible fabric based tactile sensor for closed loop control of soft robotic actuator, In proc. of 13th IEEE Conference on Automation Science and Engineering (CASE), pp. 1451–1456, 20-23 August 2017, Xi'an, China, doi: 10.1109/COASE.2017.8256308.
10. Au, A.; Bhattacharjee, N.; Horowitz, L.; Chang, T.; and Folch, A. 3D-printed microfluidic automation, Lab on a Chip, vol. 15, no. 8, pp. 1934–1941, 2015, http://doi.org/10.1039/ C5LC00126A.
11. Takenaga, S.; Schneider, B.; Erbay, E.; Biselli, M.; Scnitzler, T.; Schning, M.; T. Wagner. Fabrication of biocompatible lab-on-chip devices for biomedical applications by means of a 3D-printing process, Physica Status Solidi (a), vol. 212, no. 6, pp. 1347–1352, 2015, https://doi.org/ 10.1002/ pssa.201532053.
12. A. Kumar, "Methods and materials for smart manufacturing: additive manufacturing, Internet of Things, flexible sensors and soft robotics," Manufacturing Letters, vol. 15, Part B, pp. 122–125, 2018, doi: 10.1016/j.mfglet.2017.12.014.
13. Kim, J.; Alspach, A.; Yamane, K. 3D printed soft skin for safe human-robot interaction, In Proc. of IEEE/RSJ International Conference on Intelligent Robots and Systems (IROS), pp. 2419–2425, 28 September 2015, Hamburg, Germany, doi:10.1109/IROS.2015.7353705.
14. Agarwala, S.; Goh, G.; Yap. Y.; Goh, G.; Yu, H.; Yeong, W.; Tran, T. Development of bendable strain sensor with embedded microchannels using 3D printing, Sensors and Actuators A: Physical, vol. 263, pp. 593–599, 2017, https//doi.org/10.1016/j.sna.2017.07.025.
15. Laszczak, P.; Jiang, L.; Bader, D.; Moser, D.; Zahedi, S. Development and validation of a 3D-printed interfacial stress sensor for prosthetic applications,Medical Engineering & Physics, vol. 37, no. 1, pp. 132–137, 2015, https://doi.org/ 10.1016/j.medengphy.2014.10.002.
16. Kirthika, K.; Ponraj, G.; Ren, H. Fabrication and comparative study on sensing characteristics of soft textile layered tactile sensors, IEEE Sensors Letters, vol. 1, no. 3, pp. 1–4, 2017, doi:10.1109/LSENS.2017.2708425.
17. Kumar, K.; H. Ren, H.; Chan, Y. Soft tactile sensors for rehabilitation robotichand with 3D printed folds, In Proc of 2nd International Conference for Innovation in Biomedical Engineering and Life Sciences. ICIBEL 2017, vol. 67 of IFMBE Proceedings, pp. 55–60, Singapore, 7 December 2018, doi: 10.1007/978-981-10-7554-4_9.
18. Qiao, H.; Zhang, Y.; Huang, Z.; Wang, Y.; Li, D.; Zhou, H. 3D printing individualized triboelectric nanogenerator with macro-pattern, Nano Energy, vol. 50, pp. 126–132, 2018, https://doi.org/10.1016/j.nanoen.2018.04.071.
19. Kumar, K.; Chen, P.; Ren, H. A Review of Printable Flexible and Stretchable Tactile Sensors, Research, vol.2019, Article ID 3018568, pp. 32, 2019, https: doi.org/10.34133/2019/30188568
20. Pelrine, R.; Chiba, S. Review of Artificial Muscle Approaches, Proc. of Third Intl Symposium on Micromachine and Human Science (Invite), Nagoya, Aichi, Japan, 15-18 May, 1992, pp. 1-9.
21. Pelrine, R.; Chiba, S.; Kornbluh, R.; Eckerle. J. Artificial Muscle actuator, The first International Micromachine Symposium, Tokyo, Japan, 1-2 November 1995, pp. 1-6.
22. Chiba, S.; Waki, M. Recent Development of Dielectric Elastomers Transducers and Potential Applications, Energy and Power Engineering, vol. 15, No.2, 2023, doi: 10.4236/ epe.2023.152005.
23. Chiba, S.; Waki, M.; Ono, K.; Hatano, R.; Taniyama, Y.; Okada, E.; Ohyama, K. Challenge of creating high performance dielectric elastomers, In Proc. of SPIE2021 Smart Structures and Materials Symposium and its

23rd Electroactive Polymer Actuators and Devices (EAPAD) XXII, 115871T, Virtual Online, 22 March 2021, pp1157–1162, doi:10.1117/12.2581255.
24. Chiba, S.; Waki, M. Possibility of a Portable Power Generator Using Dielectric Elastomers and a Charging System for Secondary Batteries, Energies 2022, 15, 5854, doi:10.3390/en15165854.
25. Katchalsky, A. Rapid swelling and deswelling of reversible gels of polymeric acid by ionization. Experimentia, 5:319-320, 1949.
26. Steinberg, I.; Oplatka, A.; Katchalsky, A. Mechanochemical Engines, Nature, 210, pp. 568-517, 7 May 1966, https://www.nature.com/articles/210568a0.
27. Oguro, K.; Fujiwara, N.; Asaka, K., Onishi, K.; Sewa, S. Polymer electrolyte actuator with gold electrodes, In Proc. Smart Materials 1999, Electroactive Polymer Actuators and Devices, Newport Beach, CA, USA, Vol. 3669, 28 May 1999, doi:10.1117/12.349702.
28. Otero, T.; Sansiñena, J. Soft and wet conducting polymers for artificial muscles, Advanced Materials 10 (6), 1998, pp. 491-494, doi: 10.1002/(SICS)1521-4095(199804)10:<491:AID-ADMA491>3.0.CO;2-Q.
29. Osada, Y.; Okuzaki, H.; Hori, H. A polymer gel with electrically driven motility, Nature, Vol. 355, 1992, pp. 242-244.
30. Baughman R.; Cui, C.; Zakhidov, A.; Iqbal, Z.; Barisci, J.; Spinks, G.; Wallace, G.; Mazzoldi, A.; Rossi, D.; Rinzler, A.; Jaschinski, O.; Roth, S.; Kertesz, M. Carbon Nanotube Actuators, Science, Vol. 284, 1999, pp. 1340-1344, doi:10.1126/ science.284.5418.1340.
31. Gross, B. Experiments on Electrets, Phys. Rev. 66, 26, 1944.
32. Chou, P.; Hannaford, B. Static and dynamic characteristics of mckibben pneumatic artificial muscles, In Proc. the IEEE International Conference on Robotics and Automation, SanDiego, CA, May 8-13, 1994, p.281-286.
33. Smots, G. New developments in photochromic polymers, J. Polymers Science, Polymers Chemistry, Vol. 13 (1995) p.2223.
34. Tobushi, H.; Hayashi, S.; Kojima, S. Mechanical Properties of Shape Memory Polymer of Polyurethane Series, JSME International J., Series 1, Vol. 35, No. 3, 1992.
35. Bar-Cohen, Y. Electroactive Olymer (EAP) Actuators as Artificial Muscles – Reality Potential and Challenges, In Proc. of 19th AIAA Applied Aerodynamics Conference, Anaheim, CA, USA, June 11 2011, doi;10.2514/6.2001-149.
36. Ratna, B.; Thomsen, D.; Keller, P. Liquid crystalline elastomers as artificial muscles: role of side chain-backbone coupling, In Proc. SPIE's 8th Annual International Symposium on Smart Structure and Materials, Newport Beach, CA, USA, July 16 2001 doi:10.1117/12.432651.
37. Yuan, X.; Changgeng, S.; Yan, G.; Zhenghong, Z. Application Review of Dielectric Electroactive Polymers (DEAPs) and Piezoelectric Materials for vibration Energy Harvesting, Journal of Physics: Conference Series 744: 12-77, 2016, doi:10.1088;1742-6596/744/1/012077.
38. Chiba, S.; Waki, M. Evolving Artificial Muscles-Further Expanding Applied Technology, In Proc. of The 27th Annual Conference of the Robotics Society of Japan, Yokohama National University, Yokohama, Kanagawa, Japan, 15, September, 2009.
39. Chiba, S.; Waki, M., Dielectric Elastomer Sensor Capable of Measuring Large Deformation and Pressure, Human-Robot Interaction - Perspective and Applications, IntechOpen, December 2022, doi: http://dx.org/10.5772/intechopen.108622.
40. Waki, M.; Chiba, S. Application of Dielectric Elastomer Transducer, Chapters 5 and 2, Materials, Composition and Applied Technology of Soft Actuators, ed. K. Ataka, S & T Publishing, 2016, ISBN978-907002-61-9 C3058.
41. Chiba, S.; Waki, M.; Takeshita, M.; Uejima, M.; Arakawa, K.; Dielectric elastomer using CNT as an electrode. In Proc. SPIE 11375, Electroactive Polymer Actuators and Devices (EAPAD), XXII, 113751C, 22 April 2020, Online; doi.org/ 10.1117/ 12.12.2448512.
42. Han, M.; Lee, J.; Kim. J.; An, H.; Won Kang, S.; Jung, D.; Highly sensitive and flexible wearable pressure sensor with dielectric elastomer and carbon nanotube electrodes, Sensors and Actuators A: Physical, Volume 305, 111941, 15, April, 2020; doi.org/10.1016/j.sna.2020.111941.
43. Wilian, T.; Fasolt, B.; Motoki, P.; Rizzello, G.; Seelecke, S. Effects of Electrode Materials and Compositions on the Resistance Behavior of Dielectric Elastomer Transducers, *Polymers* ***2023****, 15(2), 310; https://doi.org/10.3390/polym15020310*.
44. Shigenune, H.; Sugano, S.; Nishitani, J.; Yamauchi, M.; Hosoya, N.; Hashimoto, S.; Maeda, S. Dielectric Elastomer Actuators with Carbon Nanotube Electrodes Painted with a Soft Brush, Actuators, 2018, 7, 51, doi:10.3390/act7030051.
45. Amjadi, M.; Jin, Y.; Yoon, Park, L. Ultra-stretchable and skin-mountable strain sensors using carbon nanotubes–Ecoflex nanocomposites, Nanotechnology 26, 2015, 375501, doi:10.1088/ 0957-4484/26/37/375501.

46. Walker, C.; Haller, M.; Orbaugh, D.; Freeman, S.; Rosset, S.; Anderson, I. Polymer Sensors for underwater robot proprioception, Sensors and Actuators A: Physical, vol. 351, March 2023, 114179, https://doi.org/10.1016/j.sna.2023.114179.
47. Rizzelllo, G. A Review of Cooperative Actuator and Sensor Systems Based on Dielectric Elastomer Transducers, *Actuators* 2023, *12*(2), 46, https:// doi.org/ 10.3390/act12020046.
48. Vennemann, N.; Kummerlowe, C.; Schneider, M.; Broker, D.; Siebert, A.; Teich, S.; Rosemann, T. Influence of unipolar electric fields on the behavior of dielectric elastomer actuators based on plasticized acrylonitrile-butadiene rubber (NBR), Journal of Applied Polymer Science, Volume 140, Issue 14, e53694, 2023, https:// doi.org/10.1002/app.53694.
49. Jung, K.; Kim, K.; Choi, H.; A self-sensing dielectric elastomer actuator, Sensors and Actuators A: Physical, Volume 143, Issue 2, 16 May 2008, Pages 343-351; doi.org/10.1016/ j.sna.2007. 10.076.
50. Bose, H.; Fub, E.; Novel dielectric elastomer sensors for compression load detection, In Proceedings, SPIE Smart Structure and Material + Nondestructive Evaluation and Health Monitoring, 905614, 8, March, 2014; San Diego, California, UAS; doi. org/ 10.1117/ 12.204513.
51. Bose, H.; Ehrlich, J.; Dielectric Elastomer sensors with Advanced Designs and Their Applications, Actuators 2023, 12, 115, https://doi. org/ 10.3390/act12030115.
52. Seelecke, S.; Neu, J.; Croce, S.; Hubertus, J.; Sechultes, G.; Rizzello, G. Dielectric Elastomer Cooperative Microactuator Systems-DECMAS, Actuators 2023, 12, 141, https://doi.org/10.3390/ act12040141.
53. Walker, C.; Andersen, I.; Monitoring diver kinematics with dielectric elastomer sensors, In Proceedings, SPIE Smart Structure and Material + Nondestructive Evaluation and Health Monitoring, 1016307, 17, April, 2017; Portland, Oregon, UAS; doi. org/ 10.1117/12.2260394.
54. Larson, C.; Spjut, J.; Knepper, R.; Shepherd. R.; A Deformable Interface for Human Touch Recognition Using Stretchable Carbon Nanotube Dielectric Elastomer Sensors and Deep Neural Networks, Soft Robotics, Vol. 6, No. 50, 4 October, 2019; https://doi.org/10.1089/soro.2018.0086.
55. Chiba, S.; Kornbluh, R.; Pelrine, R.; Waki, M.; Artificial Muscle and Their Next Generation, In Proc. International Symposium on Organic and Inorganic Electronic Materials and Related Nanotechnologies, Nagano, Nagano Pre., Japan, June 21, 2007.
56. Venkatraman, R.; Kaaya, T.; Tchipoque, H.; Cluff, K.; Asmatulu, R.; Amick, R.; Chen, Z.; Design, fabrication, and characterization of dielectric elastomer actuator enabled cuff compression device, In Proc. SPIE 12042, Electroactive Polymer Actuators and Devices (EAPAD) XXIV, 1204205, 20 April 2022, Long Beach, California, USA; https://doi.org/10.1117/12.2613250.
57. S. Chiba. Electroactive Polymer Artificial Muscle (EPAM) in Human Life Science, In Proc. of Human Life Science Forum (Invited), Osaka Intech, Osaka, Japan, pp. 1-12, October 20, 2005.
58. Chiba, S.; Waki, M.; Takeshita, M.; Yoshizawa, T. Improvement measures for components of dielectric elastomers for heavy duty uses such as robots and power assist devices, Advances in Theoretical & Computational Physics, 4 (3), 241-249, 2021, doi.org/10.33140/ATCP.04.03.08.
59. Chiba. S.; Kobayashi, M.; Qu, T.; Zhu, S.; Waki, M; Takeshita, M.; Ohyama, K. Examination of factors to improve the elongation and output of dielectric elastomers, In Proc. SPIE 12042, Electroactive Polymer Actuators and Devices (EAPAD)XXIV, 1204211, Virtual, Online, 20 April 2022; doi.org/10.1117/12.2603716.
60. Chiba, S.; Waki, M.; Takeshita, M.; Yoshizawa, T., Yoshizawa, Y.; Yoshizawa, K.; Application of Dielectric Elastomer to Actuators, Robots, Power Assist Devices, etc., Chapter 13-1, Design of conductive materials, conductivity control and latest application development, ed. K. S. Kohase, December 2021, Technical Information Institute Co., Ltd, ISBN: 978-4-86104-867-8-C3054.
61. Chiba, S.; Waki, M.; Tanaka, Y.; Tsurumi, N; Okamoto, K.; Nagase, K.; Honma, M.; Yokota, H.; Odagiri, K.; Sato, H.; Saiki, T.; Kaneko, J. Elastomer Transducers, Advances in Science and Technology, Vol. 97, pp. 61-74, 2017, Trans Tech Publications, Switzerland, doi:10.4028/ www.scientific.net/ AST.97.61.017.
62. Chiba, S.; Waki, Fujita, K.; Song, Z.; Ohyama, K.; Zhu, S.; Recent Progress on Soft Transducers for Sensor Networks, In book, Technologies and Eco-innovation towards Sustainability II (pp. 285-298), Springer Nature, 2019, doi.org/10.1007/ 978-981-13-1196-3_23.
63. Aimura, Y. Basic properties and applications of hydrogenated nitrile rubber, Journal of The Society of Rubber Science and Technology, Vol. 70, No. 12, pp. 681-688, 1997.
64. Chiba, S.; Waki, M.; Takeshita, M.; Ohyama, K. Possibilities of Artificial Muscles Using Dielectric Elastomers and their Applications, Advanced Materials Research, Vol. 1176, pp-117, 2023, Trans Tech Publication Ltd, Switzerland, ISSN:1662-8985, http://dx.doi.org/10.4028/p-jj7z4z.